Journal of Energy Technologies and Policy
ISSN 2224-3232 (Paper) ISSN 2225-0573 (Online)
Vol.6, No.6, 2016

Numerical Investigation and Improvement of Aerodynamic Performance of Savonius Wind Turbine

O. S. OLAOYE* O. ADEOYE
Department of Mechanical Engineering, Ladoke Akintola University of Technology, Ogbomoso, Oyo State, Nigeria

Abstract
Higher demand for energy has lead to increase in the consumption of conventional energy which has become more expensive and scarce. There is the need to generate power from renewable sources to reduce the demand for fossil fuels and growing concern due to increase in the effects of climate change, such as global warming and acid rain generated by extensive and deliberate use of fossil fuels in the electric generating plants and transport system. In this work, the aerodynamic characteristics of Savonius wind turbine were investigated numerically by varying the rotor configuration (semi-circular and segment of circle) and overlap ratio so as to obtain the optimum design configuration which could give better performance of Savonius rotor. Comparison between the static torque coefficient at different overlap ratios of 0%, 20%, and 40% for the two configurations were studied using Solidworks CFD software. The flow around the rotor with overlap ratio variation was analyzed with the help of velocity, pressure contours and static torque coefficient equation of the rotor. It was observed from the analysis that the overlap of 20% was the optimum overlap condition at which pressure, velocity differences and coefficient of static torque across the rotor were the highest for both configurations and that segment of a circle produced the highest characteristics for better performance.
Keywords: Overlap ratio, aerodynamic, Savonius, Static torque coefficient, rotor configuration.

1. Introduction

Due to the rising demand of energy, conventional energy is becoming more expensive and scarce. There is the need to generate energy from renewable source such as wind energy, solar energy, tidal energy, geothermal energy and biomass energy, to reduce the demand for fossil fuels which has lead to increase in the effect of climate change such as global warming and acid rain generated by extensive and deliberate use of fossil fuels mainly in the electric power generating plants and transport vehicles. Wind energy is an alternative source of energy to fossil fuels as it is renewable, readily available, widely distributed, and produces lower greenhouse gas emissions [1]. Wind turbines are generally classified into two families: horizontal axis wind turbine (HAWT) and vertical axis wind turbine (VAWT) machines. This classification refers to the position of rotor axis relative to the wind [2]. Nowadays, HAWTs are the most popular configuration because they have higher efficiency, but they are only suitable in places with extremely strong, gusty winds and urban areas [3]. In contrast, VAWTs work well in places with relatively low wind strength, and constant winds. HAWTs are highly developed and used in all large-scale wind farms [3]. VAWTs include both a drag-type configuration, such as the Savonius rotor, and a lift-type configuration, such as the Darrieus rotor [4]. Previous experimental work reveals that two blades Savonius wind turbine is more efficient than three and four blade when tested under the same condition [8, 11]. Experimentally and numerically investigations on effect of overlap ratio and Reynolds number show that at higher Reynolds number, turbine model without overlap ratio gives better aerodynamic coefficients and at low Reynolds number model with moderate overlap ratio gives better results [9]. Theoretical investigation on inclusion of curtain arrangement on a wind deflector shows that the arrangement increase and improve the power of the Savonius wind rotor and naturally its performance [10].

Studies have been carried out in wind tunnels. Generally, the global performance of a rotor, derived from the conventional Savonius rotor was presented but no parametric study was really realized. The flow which is greatly non-stationary is very complex: the aerodynamic studies are rare and old, and do not permit the prediction of the energetic behaviour of the rotor [5]. The main parameters of a Savonius turbine are given in figure 1, [6]. Three factors are identified as affecting the performance of the Savonius turbine: aspect ratio, Overlap ratio and how the rotors are stacked. Therefore in this study, aerodynamic characteristics of Savonius wind turbine were investigated numerically by varying the rotor configuration and overlap ratio for optimum design configuration and better performance of rotor to be achieved. As the blade rotates from 0^0 - 90^0 the lift force acting on the blade goes on increasing which in turn exerts tangential force on the blade [7].

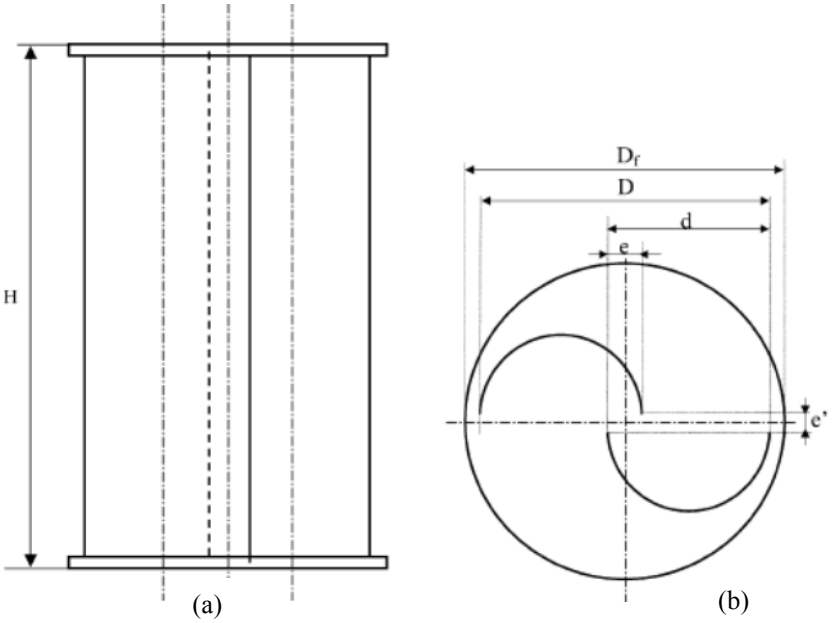

Figure 1: Schematic diagram of a single- stack Savonius, (a) Front View and (b) Top View.

2. Methodology

2.1 Physical and Computational Model

Computational domain analysis made for the physical model of the Savonius rotor was built by solidworks and simulated using solidworks flow simulation. Flow past a Savonius wind turbine was simulated by solving numerically the unsteady Navier-Stokes equation for an incompressible fluid in a two-dimensional geometry (see figures 2 and 3). A uniform velocity and default ambient condition was used at the inlet. The calculation domain was divided into two main blocks, one of which covered the area inside the rotor, and the outside of the rotor. Between these two main blocks, a sliding mesh was used which would enable accurate treatment of the rotor motion in the uniform freestream field.

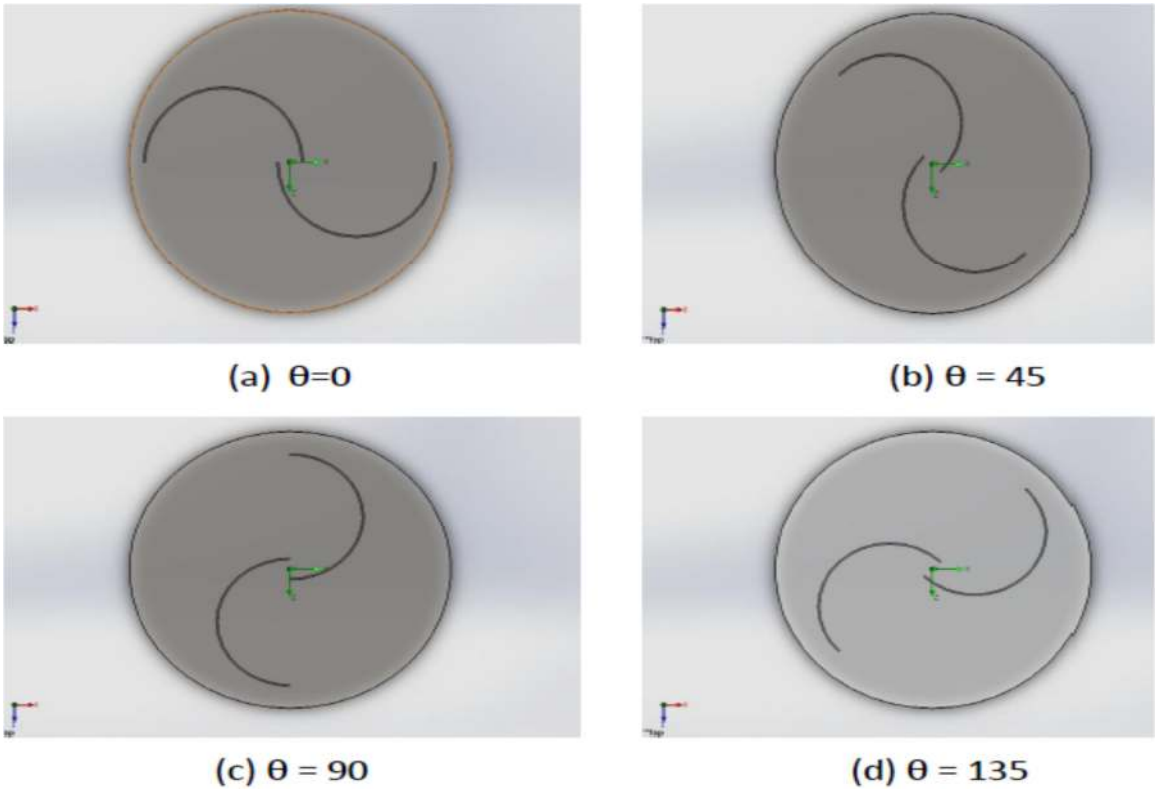

Figure 2: Differnet angles of rotation of a savonius semi-circular scoops at G=0.2.

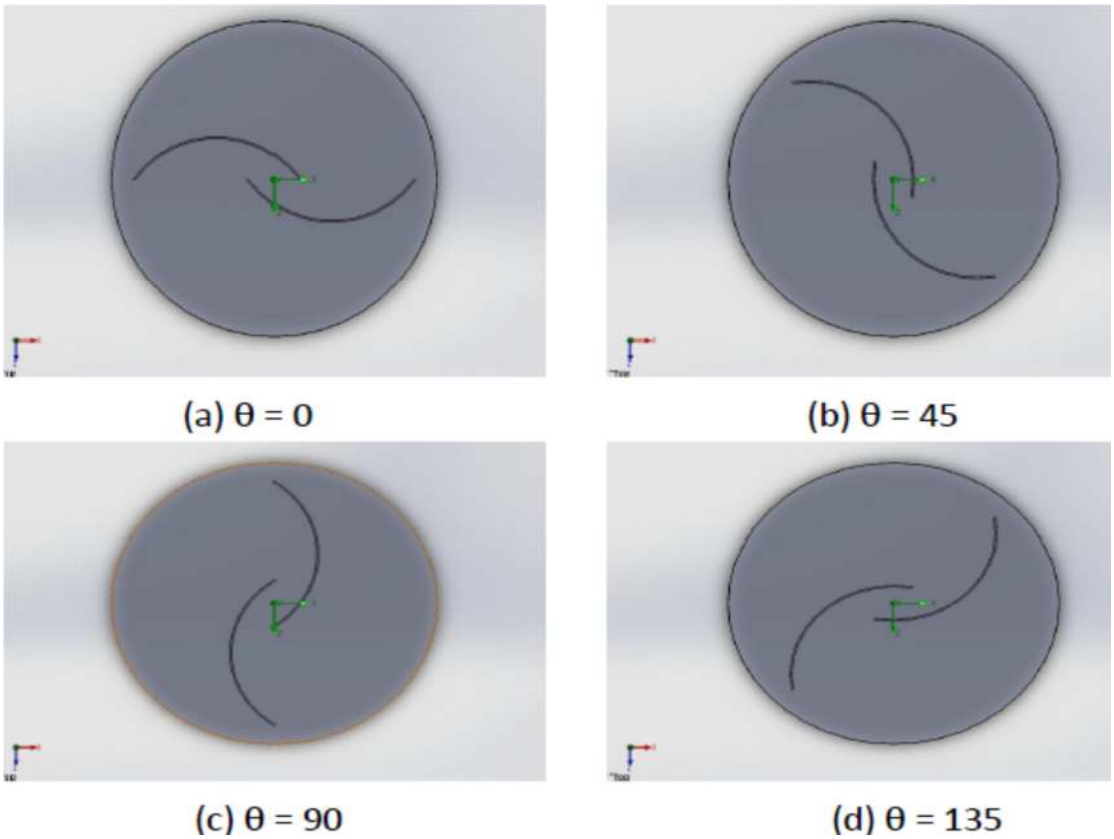

Figure 3: Different angles of rotation of a Savonius segment of circule- scoops at G=0.2.

2.2 Simulation Method

In the present study, solid works CFD software package program was used. By using it the Savonius wind rotor with different blade shape and overlap ratio have been analysed from aerodynamics aspects. Modelling of the study was done using solid work to create the model and mesh. Continuity and momentum equations were solved numerically using the CFD part of solid works software. Figure 4 shows the computational domain and boundary conditions.

Mathematical Model

Flow past the Savonius rotor was simulated by solving numerically the unsteady Navier-Stokes equation for an incompressible fluid in a two-dimensional geometry. The equations for continuity and momentum may be expressed in form as follows:

Continuity $$\frac{\partial u}{\partial x}+\frac{\partial v}{\partial y}=0 \quad (1)$$

X-momentum $$\frac{\partial u}{\partial t}+\frac{\partial}{\partial x}(uv)+\frac{\partial}{\partial y}(vu)=-\frac{\partial P}{\partial y}+\frac{1}{Re}\left(\frac{\partial^2 u}{\partial x^2}+\frac{\partial^2 u}{\partial y^2}\right) \quad (2)$$

Y-momentum $$\frac{\partial v}{\partial t}+\frac{\partial}{\partial x}(uv)+\frac{\partial}{\partial y}(vu)=-\frac{\partial P}{\partial y}+\frac{1}{Re}\left(\frac{\partial^2 v}{\partial x^2}+\frac{\partial^2 v}{\partial y^2}\right) \quad (3)$$

The governing equation that was used for the simulation is the Reynolds Averaged Navier-Stokes (RANS) equations solved by Solidworks are presented in Equations 4 and 5. The RANS approach of permitting a solution for the mean flow variables greatly reduces the computational effort. If the mean flow is steady, the governing equations will not contain time derivatives and a steady-state solution can be obtained as follows:

$$\frac{\partial \rho}{\partial t}+\frac{\partial(\rho u_i)}{\partial x_i}=0 \quad (4)$$

$$\frac{\partial(\rho u_i)}{\partial t}+\frac{\partial(\rho u_i u_j)}{\partial x_j}=\frac{\partial P}{\partial x_i}+A+B \quad (5)$$

Here, $A=\frac{\partial[\mu(\frac{\partial u_i}{\partial x_j}+\frac{\partial u_j}{\partial x_i}-\frac{2\delta_{ij}}{3}\frac{\partial u_i}{\partial x_i})]}{\partial x_j}$ and $B=\frac{\partial(-\rho\overline{u_i u_j})}{\partial x_j}$

This approach was adopted for this engineering calculation, and was used with k-ε turbulence models as shown below:

$$\frac{\partial(\rho k)}{\partial t}+\frac{\partial(\rho k u_j)}{\partial x_j}=\frac{\partial\left[\left(\mu+\frac{\mu_i}{\sigma_k}\right)\frac{\partial k}{\partial x_j}\right]}{\partial x_j}+G_k+G_b-\rho\varepsilon-Y_M+S_k \quad (6)$$

$$\frac{\partial(\rho\varepsilon)}{\partial t}+\frac{\partial(\rho\varepsilon u_j)}{\partial x_j}=\frac{\partial\left[\left(\mu+\frac{\mu_i}{\sigma_\varepsilon}\right)\frac{\partial \varepsilon}{\partial x_j}\right]}{\partial x_j}+\rho C_1 S_\varepsilon-\rho C_2\frac{\varepsilon^2}{k+\sqrt{v\varepsilon}}+C_{1\varepsilon}\frac{\varepsilon}{k}C_{3\varepsilon}G_b+S_\varepsilon \quad (7)$$

Here, $C_1=max\left[0.43,\frac{\eta}{\eta+5}\right]$, $\eta=S\frac{\kappa}{\varepsilon}$, $S=\sqrt{2S_{ij}S_{ij}}$

Here, G_k and G_b are generation of turbulent k- ε. due to mean velocity gradients and buoyancy respectively. Y_M represents the contribution of the fluctuating dilatation in compressible turbulence to the overall dissipation rate. S and $S_{\boldsymbol{\varepsilon}}$ are user-defined source terms for ε and k respectively.

In this investigation, a uniform velocity and default ambient condition was adopted at the inlet. Fluid was considered to be incompressible air with unsteady flow. Air flow over the body was governed by the Reynolds Average Navier-Stokes equation (RANS). There are several turbulence models to identify the flow behaviour around the model. Every model has some advantages and disadvantages over the other, hence it is imperative to discover which model is most suitable for finding the actual flow behaviour around the Savonius turbine model. For this work, the k- ε turbulence equation was used to solve the flow analysis. The Savonius model surface was treated as wall and no-slip condition. This model comes under two equation groups of model in which two extra quantities: turbulence kinetic energy k and its dissipation rate ϵ were to be determined for result. Transport equations for momentum and turbulence parameter were solved using quick discretization.

The use of a sliding mesh is a powerful tool for simulating flows with rotating fields. Fort his model, the overall domain was divided into two subdomains: the rotor subdomain and the stator subdomain. The rotor subdomain rotates with respect to the stationary stator subdomain. This formulation allows cells adjacent to the boundary between the subdomains to slide relative to one another, thus allowing for transient predictions of the rotor interaction with the flow field, created by the stationary stator blades. To provide the appropriate values of velocity for each subdomain, a continuity of absolute velocity was enforced at the boundary. Each cell face was converted to an interior zone. The resulting overlap between opposing interior faces produces a single interior zone. Therefore, the sliding mesh formulation offers increased accuracy with higher computational expense.

Mathematical Expression

Rotor Area: $A = D * H$ (8)

Overlap Ratio: $G=\frac{a}{2R}$ (9)

Aspect Ratio: $AR=\frac{H}{d}$ (10)

Angular Velocity: $\omega=\frac{2\pi N}{60}$ (11)

Reynolds Number: $Re = VD/\upsilon$ (12)

Tip Speed Ratio: $\lambda=\frac{\omega D}{2V}$ (13)

Torque Coefficient: $C_T = 4T/(\rho U^2 D^2 H)$ (14)

Power Coefficient: $C_T = 2T\omega/(\rho U^3 DH)$ (15)

Pressure Coefficient: $C_{Pr} = (2(P - P_a)/(\rho U^2))$ (16)

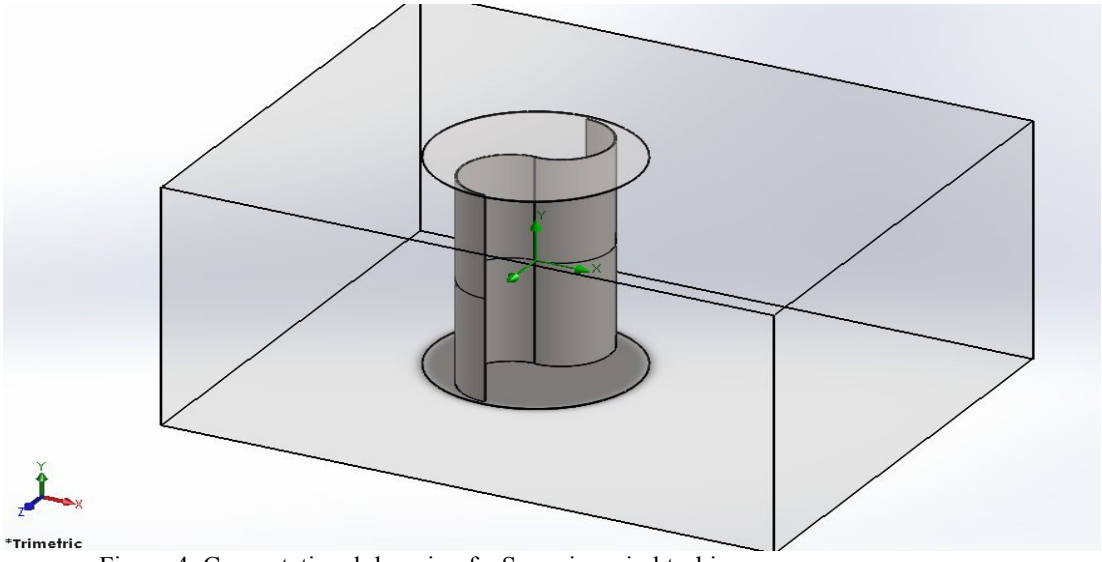

Figure 4: Computational domain of a Savonius wind turbine

2.3 Numerical Procedure

In this research, aerodynamic characteristics of a two bladed Savonius vertical wind turbine (VAWT) with different overlap ratios and configuration were investigated using numerical methods. The wind turbine was designed using solid modelling and then each part with different overlap ratio and at different angle of attack was simulated. The Savonius wind turbine height is equal to 1.4 times the outer diameter (H=1.4D) for the two different configuration. Whereas the outer diameter (D) was measured to be 1.1 times the Savonius arc diameter (d).

2D calculations was carried out using the solidworks flow simulation on the two Savonius rotor configuration with varying overlap ratio of G = 0%, 20% and 40%. The simulation was performed using the unsteady solver on moving meshes. For the two rotor configurations, the analysis type, computational domain, velocity and ambient condition are set to external, 3D domain around the rotor, 10m/s and normal atmospheric condition respectively.

3. Result and Discussion

3.1 Static Coefficient of Torque Analysis of semi-circular Savonius turbine

Figure 5 shows the distribution of static torque coefficient C_{ts} of the Savonius rotor at various overlap ratios, which were plotted against the rotor angle θ. The static torque coefficient for an overlap ratio of 0% has a maximum value of 0.01025 at a rotor angle $\theta = 60^0$ and a minimum value of -0.01691 at a rotor angle $\theta = 150^0$. At overlap ratio of 20%, static torque coefficient has a maximum value of 0.004746 and minimum value of -0.01355 at a rotor angle $\theta = 60^0$ and $\theta = 120^0$ respectively. At overlap ratio 40%, static torque coefficient has a maximum value of 0.0004823 and minimum value of -0.009809 at a rotor angle $\theta = 120^0$ and $\theta = 30^0$ respectively. This result is in line with what was obtained by [13, 14] on the relationship between overlap ratio and rotor angle. The static torque coefficient has a maximum value at small angle of attack $\theta = 30^0 - 60^0$ and a minimum value at large angle of attack $\theta = 120^0 - 150^0$. Rotor with overlap ratio of 0% produced the maximum coefficient of torque at angle $\theta = 60^0$ but looking closely at the figure rotor with overlap ratio 20% develop more positive coefficient of torque and well distributed that 0% overlap ratio.

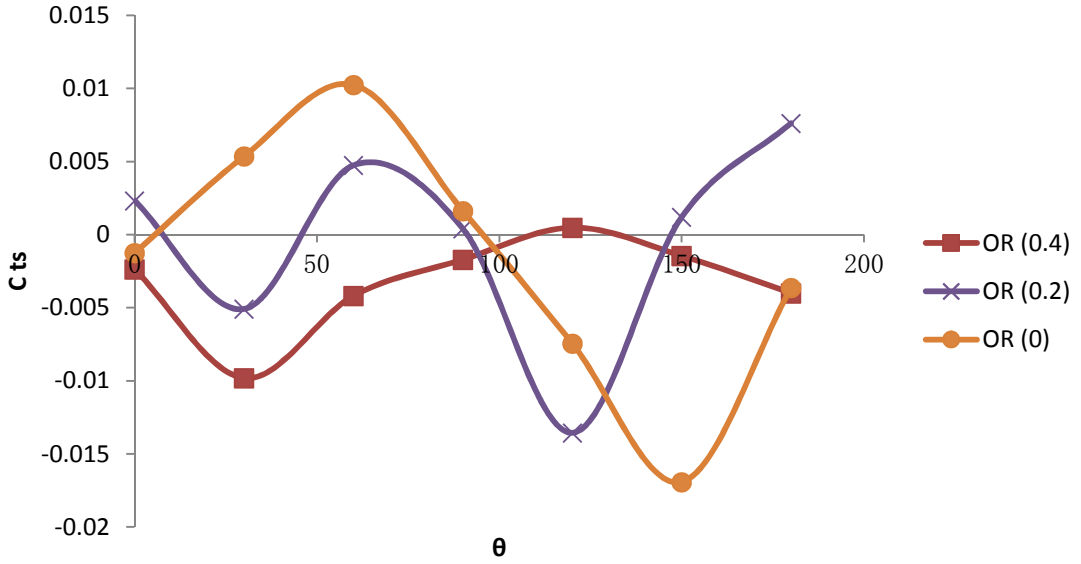

Figure5: C_{ts} against angle of attack at different angle of attack (Semi-circular Savonius rotor).

3.2 Static Coefficient of Torque Analysis of segment of circle Savonius turbine

Figure 6 shows the distribution of static torque coefficient C_{ts} of the Savonius rotor at various overlap ratios, which are plotted against the rotor angle θ. The static torque coefficient for an overlap ratio of 0% has a maximum value of 0.00894 at a rotor angle $\theta = 0^0$ and a minimum value of -0.01872 at a rotor angle $\theta = 30^0$. At overlap ratio of 20%, static torque coefficient has a maximum value of 0.01172 and minimum value of -0.00749 at a rotor angle $\theta = 120^0$ and $\theta = 90^0$ respectively. At overlap ratio 40%, static torque coefficient has a maximum value of 0.00444 and minimum value of -0.00735 at a rotor angle $\theta = 60^0$ and $\theta = 180^0$ respectively. The static torque coefficient has a maximum value at large angle of attack $\theta = 120^0$ and a minimum value at large angle of attack $\theta = 30^0$. Also maximum torque was produced at overlap ratio 20% and angle angle of attack $\theta = 120^0$

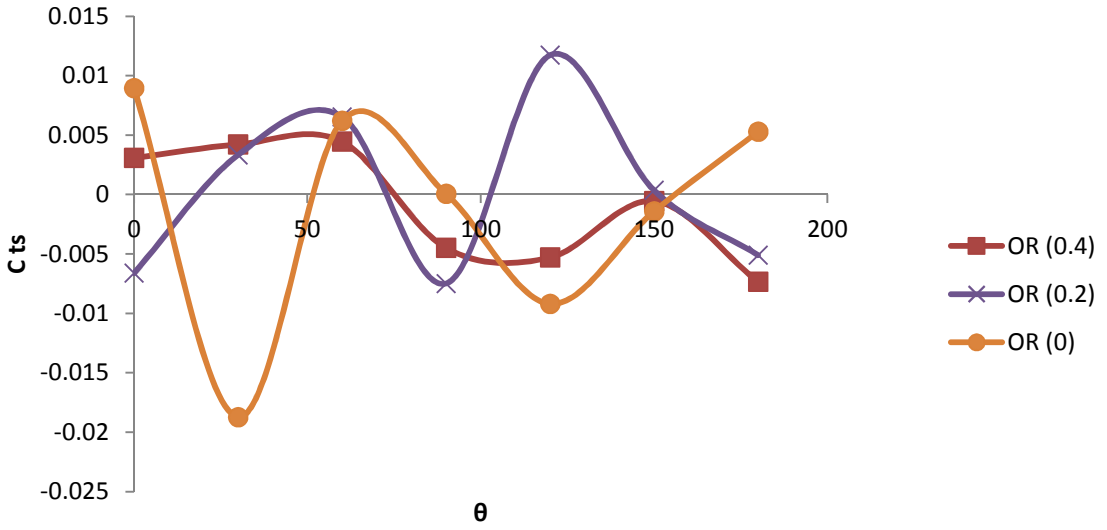

Figure 6: Graph of C_{ts} against angle of attack at different angle of attack (segment of circule Savonius rotor).

3.3 Velocity Contour Plot Analysis of semi-circular Savonius turbine

Considering the velocity distribution difference contour plots in figure 7, the velocity difference value at the three overlap ratios (40%, 20%, 0%) from upstream to the downstream side of Savonius wind rotor were analyzed. Overlap ratio of 40% gives the highest velocity at $\theta = 60^0$ and $\theta = 150^0$ angles of attack with a value of 5.899 m/s and 8.158 m/s respectively. Overlap ratio of 20% gives the highest velocity at $\theta = 30^0$ and 120^0 angles of attack with a value of 7.007 m/s and 8.662 m/s respectively. Overlap ratio of 0% gives the highest velocity difference at $\theta = 30^0$ angle of attack with a value of 7.812 m/s.

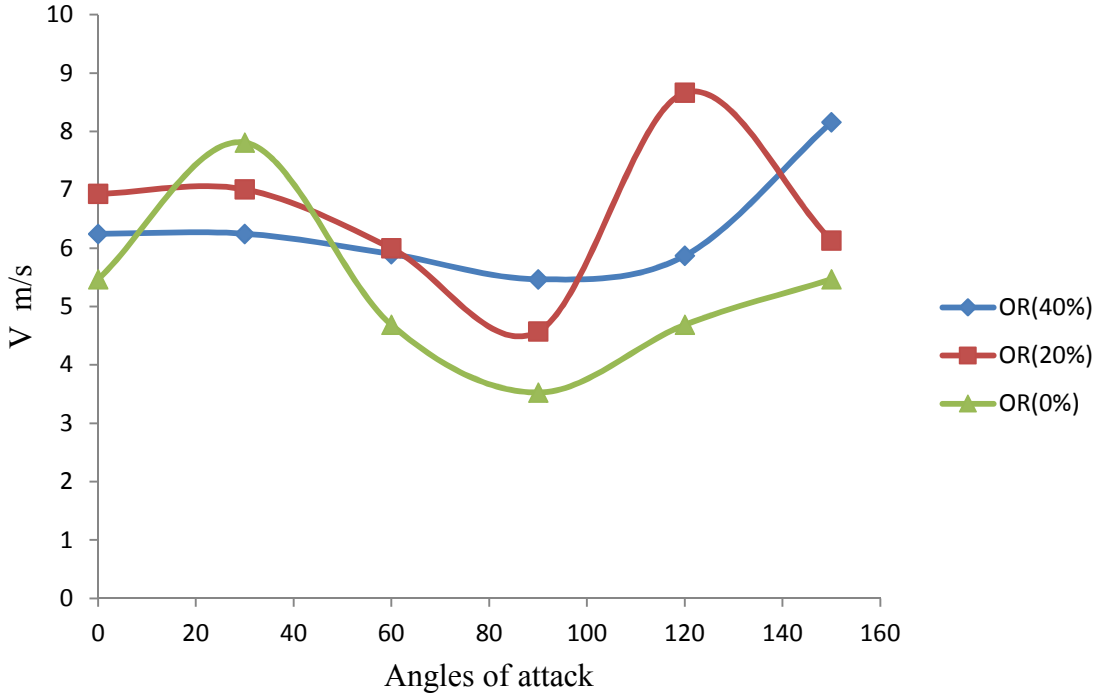

Figure 7: Velocity distribution difference between upstream and downstream region.

Rotor with overlap ratio of 20% produced the highest velocity and it was further analyzed for velocity variation from upstream to downstream at different angles. The results as in figure 8 show the distribution of velocity contour plot of the Savonius rotor at various angles of attack for an overlap ratio of 20% for semi-circular

Savonius wind turbine at an initial velocity of 10 m/s. The relative velocity magnitude contours show that there is a decrease of relative velocity magnitude from the upstream side to the downstream side of the rotor. Figure 8(a) for angle of attack = 0^0 shows that relative velocity decreases from 8.663 m/sec upstream to 1.733 m/sec downstream across the rotor. Figure 8(b) for angle of attack = 30^0 shows that it decreases from 10 m/sec upstream to 2.188 m/sec downstream across the rotor. Figure 8(c) for angle of attack = 60^0 shows that relative velocity decreases from 8.9 m/sec upstream to 2.903 m/sec downstream across the rotor. Figure 8(d) for angle of attack = 90^0 shows that it decreases from 8.548 m/sec upstream to 3.081 m/sec downstream across the rotor. Figure 8(e) for angle of attack = 120^0 shows that relative velocity decreases from 10.395 m/sec upstream to 1.733 m/sec downstream across the rotor. Figure 8(f) for angle of attack= 150^0 shows that it decreases from 9.192 m/sec upstream to 1.034 m/sec downstream across the rotor. The velocity difference attain it maximum value at 120^0 followed by 30^0 angle of attack. This implies that the power extraction from the wind by the rotor is at its peak at these angles of attack.

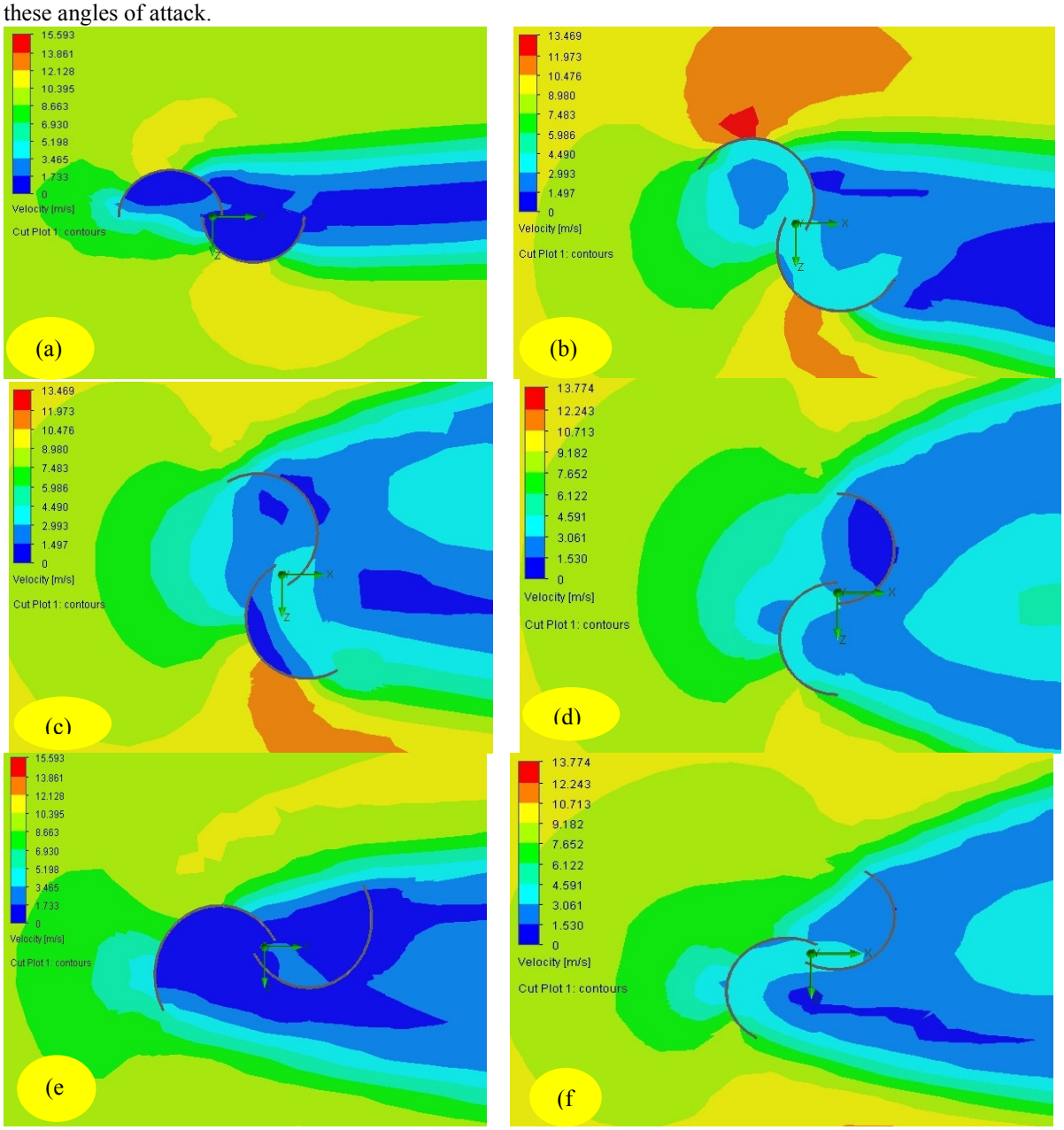

Figure 8: Velocity contour plot of semi-circular Savonius rotor at different angles of attack.

3.4 Velocity Contour Plot Analysis of segment of circle- Savonius type

Considering the velocity distribution difference contour plots in figure 9, the velocity difference value at the three overlap ratios (40%, 20%, and 0%) from upstream to the downstream side of Savonius wind rotor were analyzed. Overlap ratio of 40% gives the highest velocity at $\theta = 150^0$ angles of attack with a value of 6.442 m/s. Overlap

ratio of 20% gives the highest velocity at $\theta = 0^0$ angles of attack with a value of 7.647 m/s, and overlap ratio of 0% gives the highest velocity of 6.118 m/s at $\theta = 30^0$ angles of attack.

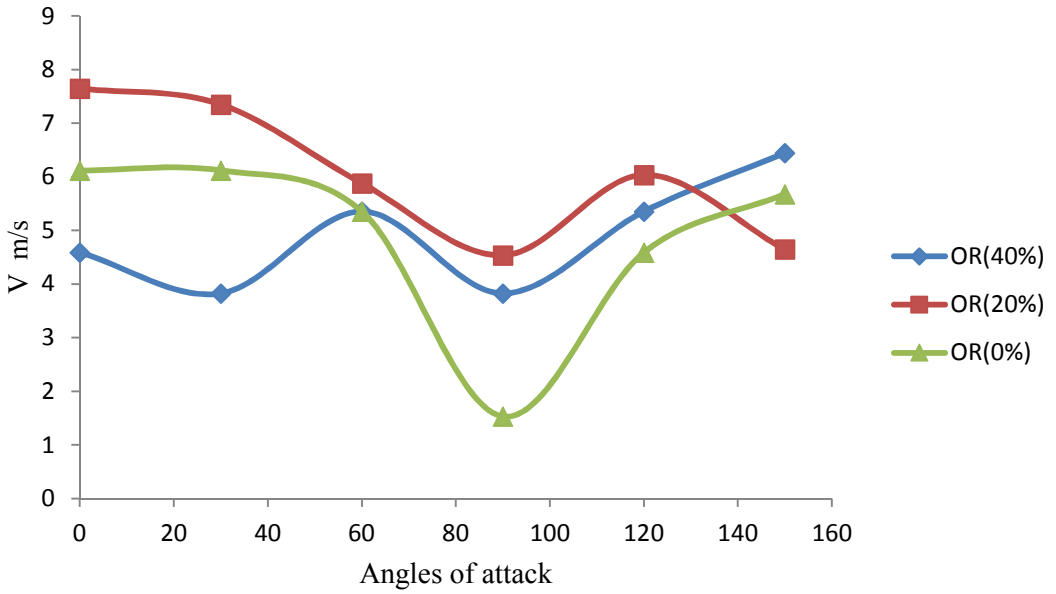

Figure 9: Velocity distribution difference between upstream and downstream region.

Rotor with overlap ratio of 20% produced the highest velocity and it was further analyzed for velocity variation from upstream to downstream at different angle. The result as in figure 10 shows the distribution of velocity contour plot of the Savonius rotor at various angles of attack for an overlap ratio of 20% for circular-segment Savonius wind turbine at an initial velocity of 10 m/s. The contour plots are obtained for angle of attacks at which static torque coefficient of the rotor is the highest for all overlap conditions. The relative velocity magnitude contours show that there is a decrease of relative velocity magnitude from the upstream side to the downstream side of the rotor. Figure 10(a) for angle of attack = 0^0 shows that relative velocity decreases from 9.176 m/sec upstream to 1.529 m/sec downstream across the rotor. Figure 10(b) for angle of attack = 30^0 shows that it decreases from 10.289 m/sec upstream to 2.94 m/sec downstream across the rotor. Figure 10(c) for angle of attack = 60^0 shows that relative velocity decreases from 8.819 m/sec upstream to 2.94 m/sec downstream across the rotor. Figure 10(d) for angle of attack = 90^0 shows that it decreases from 7.557 m/sec upstream to 3.023 m/sec downstream across the rotor. Figure 10(e) for angle of attack = 120^0 shows that relative velocity decreases from 9.058 m/sec upstream to 3.023 m/sec downstream across the rotor. Figure 10(f) for angle of attack= 150^0 shows that it decreases from 9.539 m/sec upstream to 4.894 m/sec downstream across the rotor. The velocity difference attain it maximum value at 0^0 and 30^0 angle of attack. This implies that the power extraction from the wind by the rotor is at its peak at these angles of attack.

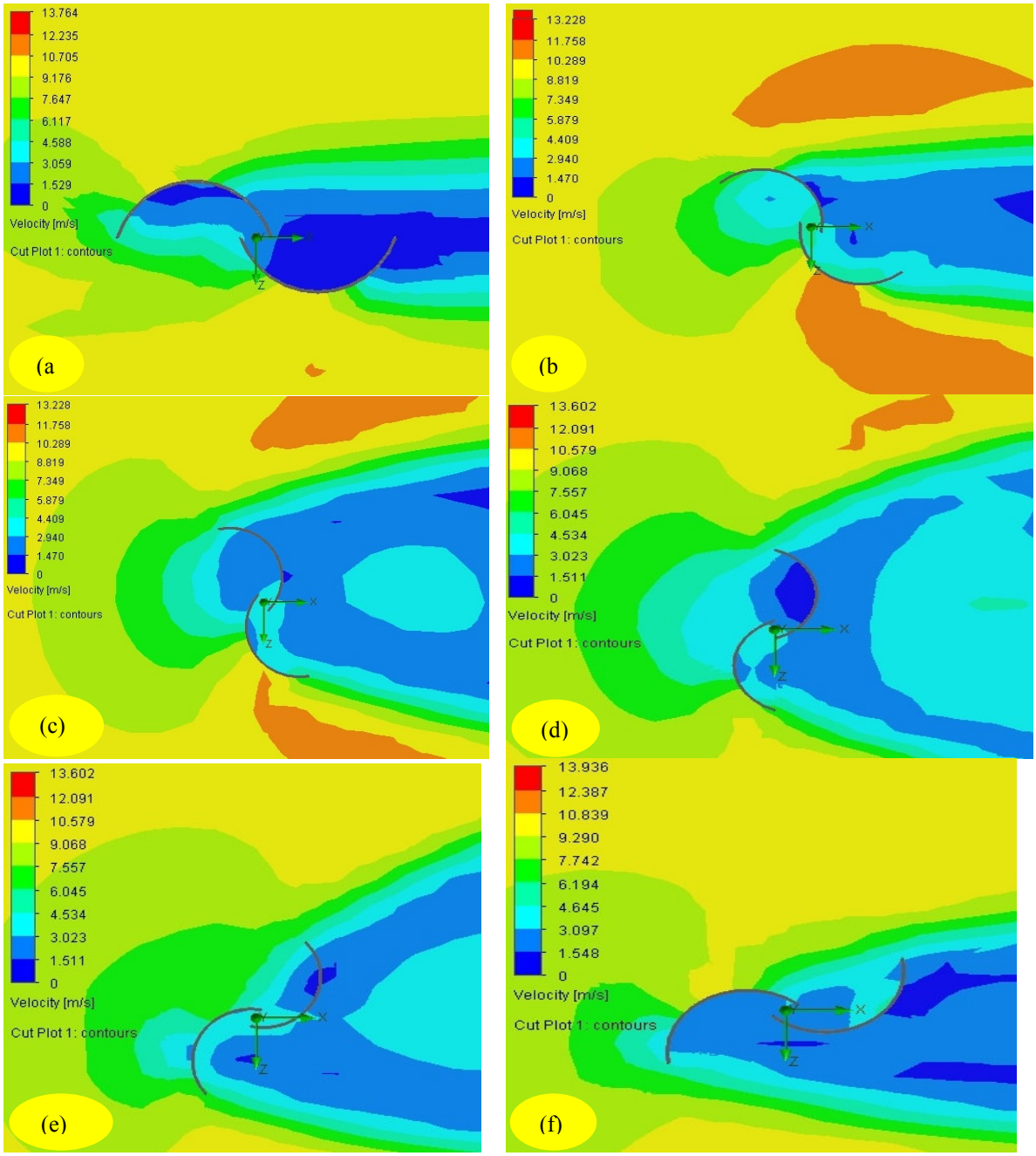

Figure 10: Velocity contour plot of segment of circle Savonius rotor at different angles of attack.

4. CONCLUSION

The following can be concluded from work:

1. The static torque coefficient and velocity distribution against the angle of attack show that for both semi-circular Savonius and segment of a circle Savonius wind turbines overlap ratio of 20% gave maximum coefficients of torque and good velocity extraction. Therefore, overlap condition of 20% is the optimum overlap in terms of coefficient of torque and velocity variations for which performance of the Savonius rotor is also at the best. Segment of a circle gave the maximum coefficient of torque and will be the best option.
2. For the two configurations at overlap ratio of 20%, the velocity difference attains its maximum value at 30^0 and 120^0 angle of attack (i.e maximum lift). This implies that the power extraction from the wind by the rotor is at its peak at these angles of attack.

Reference

1. Mohammed H.A., Experimental Comparison Study for Savonius Wind Turbine of Two & Three Blades

at Low Wind Speed. International Journal of Modern Engineering Research (IJMER). Vol. 3, Issue. 5, pp-2978-2986 (2013).

2. Ivan, D., Fawaz, M., Exploring the Flow around a Savonius Wind Turbine. Energy Procedia. Arts et Metiers Paris Tech, 151, bd de L'Hopital, 75013 Paris France, Pp. 1-9 (2012).
3. Sharma, K.K., Gupta, R., Physics of a three-Bucket Savonius Rotor using Computational Fluid Dynamics (CFD). International Journal of Applied Engineering Research. Dept. of Mechanical Engineering, N.I.T. Silchar. ISSN 0973-4562, Volume 8, Number 15, pp. 1773-1782 (2013).
4. Khandakar, N.M., Experimental and Numerical Investigation on Aerodynamic Characteristics of Savonius Wind Turbine with various Overlap Ratios. Georgia Southern University. Electronic Theses & Dissertations. Paper 773, pp. 1-89 (2010).
5. Menet, J.-L., Nachida, B. :Increase in the Savonius Rotors Efficiency via Parametric Investigation. Université de Valenciennes - Le Mont Houy, F-59313, Valenciennes, Cedex 9, France. Pp. 1-11 (2010)
6. Yaakob O.B., Tawi, K.B., Sunanto, D.T.S., Computer simulation studies on the effect overlap ratio for savonius type vertical axis marine current turbine. Department of Marine Technology, Universiti Teknologi Malaysia, pp. 79-88 (2010).
7. Abhijeet, M.M., Prashant, M.P., Analysis of Lift and Drag Forces at Different Azimuth Angle of Innovative Vertical Axis Wind Turbine. International Journal of Energy and Power Engineering .Special Issue: Energy Systems and Developments. Vol. 4, No. 5-1, pp. 12-16. doi: 10.11648/j.ijepe.s.2015040501.12 (2015).
8. Mohammed, H.A. (2013) Experimental comparison study for Savonius wind Turbine of two and three blades at low wind speed. International Journal of Modern Engineering Research (IJMER) vol.3 issue 5 pp2978 – 2986.
9. Morshed, K.N. (2010) Experimental and Numerical investigations on aerodynamic characteristics of Savonius wind turbine with various overlap ratios. Electronic eses and Disertation paper 773 Georgia Southern University.
10. Altan, B.D and Atalgan, M (2012). A study on increasing the performance of Savonius wind rotors. Journal of mechanical Science and Technology. 26(5) pp1493-1499
11. Kadam,A.A and Patil,S.S. A review study on Savonius wind rotors for accessing the power performance. IOSR Journal of Mechanical and Civil Engineering (IOSR-JMCE) pp18-24
12. Simulation study on the performance of vertical axis wind turbine – Nor fzarizam, Bin H.J. Samiran. An M.Sc thesis submitted to Faculty of Mechanical and Manufacturing, University of Malaysia (2013)
13. Yaakob, O.B., Tawi, K.B and Sunanto, D.T.S. (2009) Computer Simulation studies on the effect of overlap ratio for Savonius type vertical axis marine current turbine. IJE transactions vol.23: pp79-88
14. Sargolzae, J and Kianifa, A. (2009). Modelling and Simulationof wind turbine Savonius rotors using artificial neural networks for estimation of the power ratio and torque. Simulation modeling practice and theory 17(2009) 1290 -1298